Letter

Entangled-State Time Multiplexing for Multiphoton Entanglement Generation

Zhibo Hou,[1,2,3,†] Jun-Feng Tang,[1,2,†] Chang-Jiang Huang,[1,2] Yun-Feng Huang,[1,2,3] Guo-Yong Xiang,[1,2,3,*] Chuan-Feng Li,[1,2,3] and Guang-Can Guo[1,2,3]

[1] *Chinese Academy of Sciences (CAS) Key Laboratory of Quantum Information, University of Science and Technology of China, Hefei 230026, People's Republic of China*

[2] *CAS Center for Excellence in Quantum Information and Quantum Physics, University of Science and Technology of China, Hefei 230026, People's Republic of China*

[3] *Hefei National Laboratory, University of Science and Technology of China (USTC), Hefei 230088, People's Republic of China*

(Received 13 March 2022; revised 12 October 2022; accepted 8 December 2022; published 24 January 2023)

Large-scale quantum entanglement endows quantum technologies with significant quantum advantages over their classical counterparts. Nevertheless, this power is rarely unleashed due to our practical inefficiency in generating multiphoton entanglement. Here, we implement an active entangled-state time-multiplexing method, which can generate $2n$-photon entangled states with an exponential efficiency-enhancement factor of B^{n-1}. We experimentally achieve a multiplexing power of $B = 6.43$ in preparing four-photon Greenberger-Horne-Zeilinger states with fidelities above 0.806(5), which is mainly limited by technical loss in multiplexing. Even with current multiplexing power, our method can readily boost the efficiency of preparing 12-photon entangled sources by a factor of $6.43^5 \approx 10^4$. Our work demonstrates that entangled-state time multiplexing promises a path toward efficiently preparing and harnessing multiphoton quantum entanglement for unprecedented large-scale quantum computation and high-precision quantum metrology.

DOI: 10.1103/PhysRevApplied.19.L011002

Introduction—Quantum entanglement powers quantum information processing tasks with better security, efficiency, and precision [1–4]. The key to harnessing these quantum advantages lies in our capacity to generate large-scale quantum entanglement. In particular, spontaneous parametric down-conversion (SPDC) is one of the most widely used methods to prepare multiphoton entangled states [5–7] and find applications from foundational studies of quantum nonlocality [8–11] to quantum information tasks of quantum communication [12,13], quantum computation [14,15], and quantum metrology [16–19]. In the SPDC process, a pair of photons are generated with probability p in each pumping pulse with pumping rate R_p (period of τ). To generate $2n$-photon states, n independent photon pairs need to coincide, which succeeds with an exponentially decreasing probability p^n and at a generation rate $C_0 = R_p p^n$. To date, the state-of-art photonic system is a 12-photon entangled source with a brightness of 1 count/h [20].

A time-multiplexing method is proposed to solve the probabilistic problem of the SPDC source [21–23]. The key idea is to extract and use the temporal information about the pulse with which the photon pair is generated. It is only very recently that the single-photon time-multiplexing method (STM), which aims to prepare on-demand single-photon sources, has achieved experimental advances [24–26]. However, the long-sought-after entangled-state time multiplexing (ETM) is much more challenging and has barely been explored [22,27], mainly because entanglement is fragile and easily destroyed when using STM techniques [24–26].

By using polarization-independent optical switches to preserve entanglement in multiplexing, we propose and implement an ETM method that can significantly boost the generation efficiency of large-scale entanglement. Moreover, our ETM method can be conveniently adapted from the conventional multiphoton-SPDC scheme in Fig. 1(a) just by adding dynamic delay lines for all signal photons immediately before the multiphoton-interference stage, as illustrated in Fig. 1(b). Technical imperfections, such as the finite multiplexing rate, the practical loss, and the dead time of the dynamic delay lines, can significantly undermine the efficiency enhancement of ideal ETM. We change the multiplexing process from Figs. 1(c) and 1(d) to modify the ideal ETM as a practical ETM, which is similar to relative time multiplexing [28]. This is more robust against practical imperfections than ideal ETM and saves one dynamic delay line for the last photon in Fig. 1(b). We then implement this practical ETM to generate four-photon Greenberger-Horne-Zeilinger (GHZ) states with fidelities above 0.806 and experimentally achieve a time-multiplexing power of 6.43, which is mainly limited by

*gyxiang@ustc.edu.cn
†These authors contributed equally to this work.

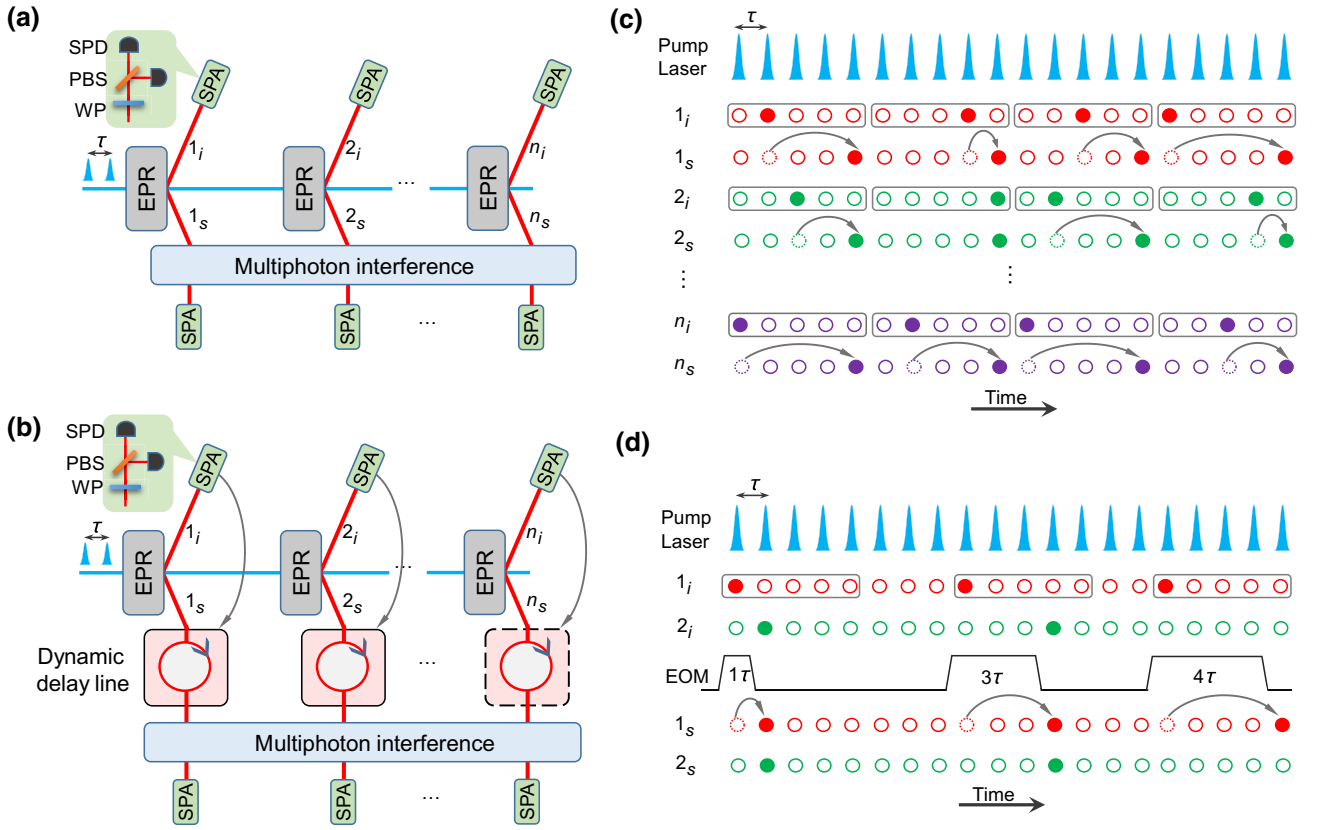

FIG. 1. A conventional and an entangled-state time-multiplexing scheme for generating multiphoton polarization-entangled states. (a) The conventional scheme, which first generates n independent EPR-entangled photon pairs and then uses multiphoton interference between the n signal photons to entangle the $2n$ photons. (b) The entangled-state time-multiplexing scheme, which has an extra module of dynamic delay lines to each signal photon before multiphoton interference. For practical ETM, the last dynamic delay line (dashed box) for signal photon n_s can be saved. (c) The time-multiplexing process for ideal ETM, which shifts all the n signal photons to the same position regardless of their generation positions every N pulses ($N = 5$ in the figure). (d) The time-multiplexing process of practical ETM for $N = 5$ and $n = 2$. It is only when idler photon 1_i is detected that the first signal photon 1_s is shifted to the generation pulse of the signal photon 2_s if within the range of N pulses, instead of a fixed position or a fixed multiplexing time. EPR, Einstein-Podolsky-Rosen entangled pair; EOM, electro-optic modulator; SPA, single-photon analyzer; SPD, single-photon detector; PBS, polarizing beam splitter.

the loss in the dynamic delay line. Our experiments are implemented on a free-space photonic platform with a delay-line transmittance of 0.867, which is more desirable for implementation on the more compact and stable integrated photonic system when the loss problem can be solved (transmittance 0.1 in Ref. [29]).

Entangled-state time multiplexing for multiphoton polarization-entangled states—The entangled-state time-multiplexing method, which aims to prepare $2n$-photon entangled states efficiently, is shown in Fig. 1(b). Compared with the conventional method [7,20] shown in Fig. 1(a), it inserts an extra module of dynamic delay lines between the two modules of generating n independent EPR pairs and entangling them via multiphoton interference among the n signal photons. The inserted dynamic delay lines can actively shift the n signal photons (1_b,2_b, $\cdots$, n_b) to a fixed position (usually the last pulse) in a train of N pulses [$N = 5$ in Fig. 1(c)] by imposing on the signal photons a dynamic delay $(N - m)\tau$, which is the distance between the last pulse N and the actual generation pulse m. The actual generation pulse m is obtained by measuring the temporal information of its twin idler photons. After the delay line, the n signal photons can arrive at the multiphoton-interference module simultaneously even if generated at different pulses, yielding an exponentially boosted coincidence possibility $N^n p^n$. With an ideal multiplexing rate R_p/N, the generation rate is increased from the conventional $C_0 = R_p p^n$ to $N^{n-1}C_0$, i.e., by a factor of N^{n-1}. In this ideal scenario, the multiplexing power is determined by the number of the pulses N that we can multiplex. However, the enhancement factor of ETM can be seriously undermined in practice by the low multiplexing rate, the inevitable loss, and the dead time of the dynamical delay lines. Given a multiplexing rate R_m, a transmission efficiency η for delay τ, and a dead time $T_d = 1/R_m - N\tau$

in one multiplexing cycle $1/R_m$, the enhancement factor is reduced to $(R_m/R_p)B^n$, where $B = \eta(1-\eta^N)/(1-\eta) \leq N \leq R_p/R_m$ is the actual multiplexing power.

Practical ETM eases the detrimental effects of the low multiplexing rate and the dead time by replacing the fixed multiplexing starting points of every $1/R_m$ in Fig. 1(c) with dynamic starting points when one of the first $n-1$ signal photons occurs in Fig. 1(d). Practical ETM can save the dynamic delay line for the last photon by dynamically delaying all the first $n-1$ signal photons to the last signal photon instead of a fixed position in ETM, as shown in Fig. 1(d), which also reduces the loss effect. Thus the generation rate of practical ETM is $(1-pR_p/R_m)B^{n-1}C_0$, with improvement factors of $(1-pR_p/R_m)B^{n-1}$ over the conventional method and of $R_p(1-pR_p/R_m)/(R_mB)$ over ETM with practical imperfections. As p is usually set small (10^{-4} in our experiment) to avoid multiphoton noise, the coefficient $1-pR_p/R_m$ is close to 1 and thus the exponential enhancement factor B^{n-1} is mainly determined by B, the multiplexing power of one dynamic delay line. In the following experiment, we focus on demonstrating the multiplexing power B of one dynamic delay line in preparing four-photon GHZ states.

Experimental setup—The experimental setup is shown in Fig. 2. It comprises two polarization-entangled EPR photon pairs (gray region), a dynamic delay line (red region), and a multiphoton-interference module (blue region). The two EPR sources are created by a beamlike spontaneous parametric down-conversion (SPDC) process [30]. The pumping beam is up-converted from a pulsed Ti:sapphire laser with a wavelength centered around 780 nm, a repetition rate $R_p = 76.11$ MHz, and a pulse duration of about 150 fs. To suppress the multiphoton emission noise, relatively low pump powers are used: 30 mW for source 1 and 14 mW for source 2. Interference filters with 2-nm and 8-nm full width at half maximum (FWHM) are used for idler photons (1_i, 2_i) and signal photons (1_s, 2_s) to balance the trade-off between heralding efficiency and photon indistinguishability. The detection efficiency of the avalanche photodiode detector (SPCM-800-14-FC, Excelitas Technologies) is approximately 0.6. The overall heralding efficiency of the entangled source is 0.22. The idler photons 1_i and 2_i are measured to extract the time information about their twin signal photons 1_s and 2_s. The signal photon 1_s is directed to the dynamic delay line via a 25-m single-mode fiber. After a dynamic delay, the signal photon 1_s is then sent into the multiphoton-interference module to interfere with signal photon 2_s, which passes through another 25-m single-mode fiber. The two 25-m single-mode fibers are used to generate a fixed delay of 125 ns to compensate for the electronic latency. Finally, the multiphoton-interference module entangles the two EPR pairs to generate four-photon GHZ states.

The dynamic delay line is the key module of ETM, which in our experiment is realized by putting an optical switch with $R_m = 600$ KHz into a cavity, the one-round cavity length of which is set as the period $\tau = 13.139$ ns of the pumping pulses. The dynamic delay is realized by

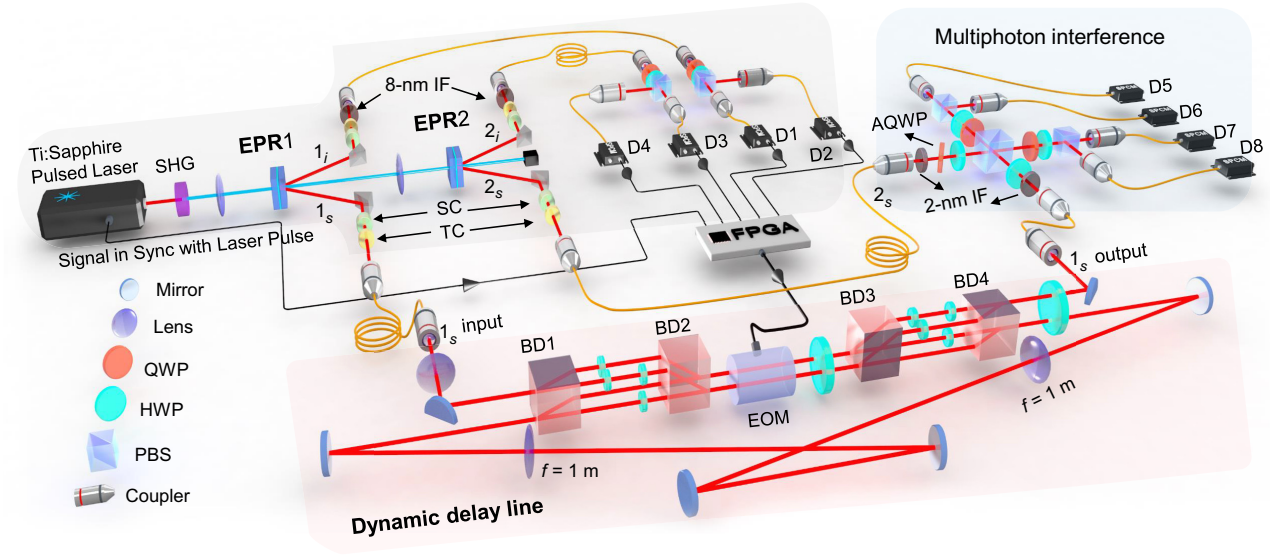

FIG. 2. The experimental setup of practical entangled-state time multiplexing. First, two polarization-entangled EPR pairs are generated and photon 1_s from EPR1 is time multiplexed in the dynamic delay line. The HWPs in the delay line are all set to 45°. Finally, the two signal photons are directed into the multiphoton-interference module to generate four-photon entanglement. Key to components: SHG, second-harmonic generation; SC, spatial compensation ($LiNbO_3$); TC, temporal compensation (YVO_4); HWP, half-wave plate; QWP, quarter-wave plate; AQWP, adjustable quarter-wave plate (phase adjustment); IF, interference filter; PBS, polarizing beam splitter; BD, beam displacer; FPGA, field-programmable gate array; EOM, electro-optic modulator.

controlling the number of loops in the cavity using the optical switch. The two lens with 1.0-m focus length in the cavity are carefully positioned to make the Gaussian spatial mode self-reproductive after one loop. The optical switch is composed of one electro-optic modulator (EOM) (EKSMA Optics; rise and fall time 6 ns, clear aperture 3.5 mm × 3.5 mm, repetition rate 600 kHz), with four beam displacers (BDs) and ten half-wave plates (HWPs). The polarization-independent feature of the optical switch to preserve entanglement is achieved by coherent conversion between the polarization degree of freedom (DOF) and the path DOF of the photon (see Ref. [31]; see also the Supplemental Material [32]). When detector D1 or D2 is triggered by the photon 1_i, the FPGA control system first sends a half-wave voltage pulse to the EOM to close the cavity immediately after photon 1_s enters the cavity. The photon will then be delayed in the cavity until the FPGA program opens the cavity when the photon pair of source 2 is generated according to the detector signal from D3 or D4 or the delay time reaches $N\tau$.

Experimental results—The experimental performance of practical ETM is mainly characterized in terms of its multiplexing power B and its effects on the quality of the entangled states. To show the multiplexing power, we plot the fourfold coincidence counts of the four-photon entangled source with respect to the multiplexed time slots N for a 300-s collection time in Fig. 3(a). We successfully multiplex up to $N = 30$ time slots with 1812 fourfold coincident counts, which is 7.5 times larger than the 241 counts with multiplexing slot $N = 1$. This multiplexing power is fitted to be $B = 6.43$ with a corresponding fitted transmission efficiency $\eta = 0.867(5)$, which, unsurprisingly, is smaller than the number of multiplexed time slots $N = 30$ because of the loss in the delay line. The loss comes not only from the imperfect transmittance of the optical components, including $T_{\mathrm{BD}} = 0.985$, $T_{\mathrm{EOM}} = 0.994$, $T_{\mathrm{HWP}} = 0.998$, $T_{\mathrm{lens}} = 0.998$, and $T_{\mathrm{mirror}} = 0.998$, but also from the non-negligible rise time (6 ns) and the uncertainties (1.5%) in the switching EOM voltages.

We then show the effects of practical ETM on the quality of the entangled states using both the Hong-Ou-Mandel interference (HOMI) visibility and the fidelity with the ideal GHZ states. The experimental results for the HOMI visibility are plotted with respect to the multiplexed time slots N in Fig. 3(b) and the three insets show three specific cases of $N = 1$, 10, and 30. As N goes from 1 to 30, the experimental HOMI visibility between sources 1 and 2 gradually decreases from 0.917(15) to 0.783(8), while, in principle, signal photons generated at different pulses enjoy very good indistinguishable properties [24,26,33–35]. The drop in the HOMI visibility mainly comes from the chromatic dispersion from the beam displacers and the EOM crystal. The total group-delay dispersion (GDD) adds up to $\varphi_{\mathrm{cycle}} \approx 1.25 \times 10^{-2}$ ps^2 per cycle in the cavity, which is relatively high compared to the 1.0-ps photon coherence time (see the Supplemental Material [32]).

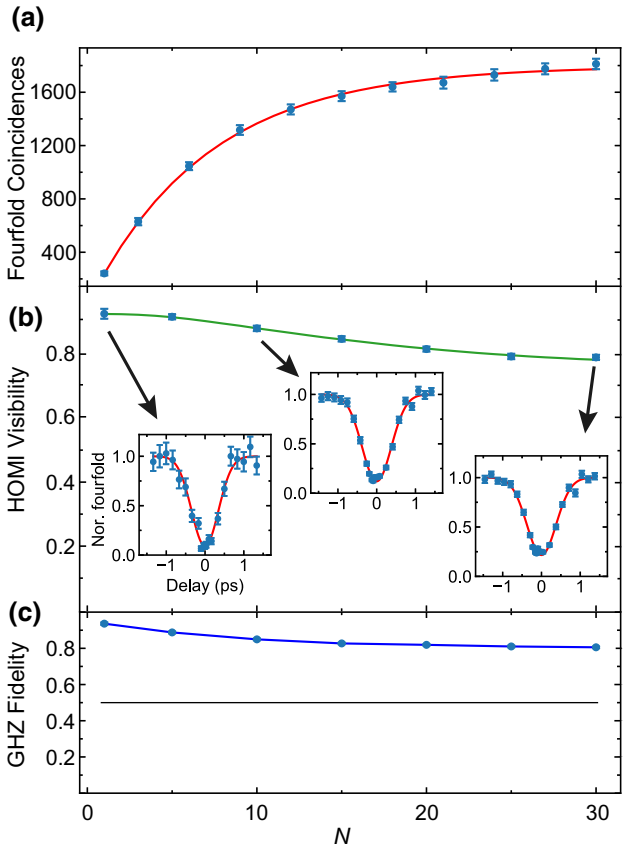

FIG. 3. The experimental results for practical entangled-state time multiplexing. (a) The fourfold coincidence counts C_N collected in 300 s versus the number of multiplexed time slots N. The red curve is fitted by the sum of the geometric sequence $C_N = C_0\eta 1 - \eta^N/1 - \eta$, with $C_0 = 276$ fitted nonmultiplexed counts and the transmittance of the cavity $\eta = 0.867$. (b) The HOMI visibility versus the number of multiplexed time slots N. The green curve is fitted by Eq. (4) in the Supplemental Material [32]. The three insets show the HOM interference between SPDC entangled sources 1 and 2 under $N = 1$, 10, and 30 time slots. The fourfold coincidence counts are normalized by the fitted maximum counts. The red curves are fitted by Gaussian distribution. (c) The measured fidelities (blue dots) of the four-photon GHZ states versus N, well above the threshold 0.5 (black line). The measurements in all subfigures are repeated 10 times, with the mean results plotted as dots and the standard deviation of the mean plotted as error bars. Nor. fourfold, normalized fourfold.

The effects of practical ETM on the fidelity of the generated four-photon GHZ state, $(|H\rangle^{\otimes 4} + |V\rangle^{\otimes 4})/\sqrt{2}$, are illustrated in Fig. 3(c) with respect to the multiplexed time slots N. The fidelities are measured using witness measurement operators $F = 1/2 - \langle W_{G_4}\rangle$ with $W_{G_4} = I/2 - |G_4\rangle\langle G_4| = I/2 - A/2 - 1/4\sum_{k=0}^{3}(-1)^k M_k$, where $A = (|H\rangle\langle H|)^{\otimes 4} + (|V\rangle\langle V|)^{\otimes 4}$ and $M_k = [\cos(k\pi/4)\sigma_x + \sin(k\pi/4)\sigma_y]^{\otimes 4}$, $(k = 0, 1, 2, 3)$. As N goes from 1 to 30, the fidelity drops from 0.936(7) to 0.806(5) but is still

much higher than the four-qubit entanglement threshold of 0.5 (black line). This fidelity drop also mainly comes from the same GDD problem as the HOMI visibility. By nullifying the GDD effect, such as by replacing the entangled sources with narrow-bandwidth ones [36] or using dispersionless optical components, the effects of practical ETM on the quality of the entangled states can be removed.

Discussion—Unlike the conventional multiphoton entangled states, the idlers of the ETM states are measured at the start of the multiplexing and thus are not suitable for tasks that need nonlocal interactions with idlers. Thus, ETM is fit for quantum information processing tasks where half of the photons (idlers) do not interact with the other photons, such as quantum metrology [37,38] or one-way quantum computation [4,39]. For these tasks, the idlers are measured not only to extract temporal information for starting multiplexing but also to record the quantum measurement results (i.e., which states the idlers collapse). The recorded measurement results for the idlers together with the later results for the signals constitute the measurement results for the entangled idlers and the signals for the quantum information processing tasks.

Conclusions—In summary, we propose an entangled-state time-multiplexing method to exponentially enhance the generation efficiency of multiphoton entangled states by using a polarization-independent optical switch in a cavity as a dynamic delay line. We experimentally implement practical ETM to generate four-photon GHZ states and demonstrate a multiplexing power of $B = 6.43$ of the dynamic delay line. Even with the currently demonstrated multiplexing power, the application of our method in the state-of-art 12-photon GHZ states in Ref. [20] would yield an enhancement factor of 10^4. By further reducing the loss in the dynamic delay line, our entangled-state time-multiplexing method promises to open up new possibilities for the large-scale quantum information tasks of quantum computation, quantum metrology, and also foundational studies of quantum physics.

Acknowledgments—The work is supported by the National Key Research and Development Program of China (Grant No. 2018YFA0306400), the National Natural Science Foundation of China (Grants No. 62222512, 12104439, 12134014, 61905234, and 11974335), the CAS Key Research Program of Frontier Sciences (Grant No. QYZDYSSW-SLH003), the Anhui Provincial Natural Science Foundation (Grant No. 2208085J03), the USTC Research Funds of the Double First-Class Initiative (Grants No. YD2030002007 and YD2030002011), and the Fundamental Research Funds for the Central Universities (Grant No. WK2470000035).

Note added.—Recently, we have become aware of the work in Ref. [40], which also uses entangled-state time multiplexing to generate scalable multiphoton entangled states. The main difference lies in the polarization-independent switching structure: we use stable interference of the beam displacers, while the work in Ref. [40] uses Sagnac interferometers.

[1] M. A. Nielsen and I. L. Chuang, *Quantum Computation and Quantum Information* (Cambridge University Press, Cambridge, United Kingdom, 2000).
[2] N. Gisin, G. Ribordy, W. Tittel, and H. Zbinden, Quantum cryptography, Rev. Mod. Phys. **74**, 145 (2002).
[3] V. Giovannetti, S. Lloyd, and L. Maccone, Advances in quantum metrology, Nat. Photon. **5**, 222 (2011).
[4] R. Raussendorf and H. J. Briegel, A One-Way Quantum Computer, Phys. Rev. Lett. **86**, 5188 (2001).
[5] P. G. Kwiat, K. Mattle, H. Weinfurter, A. Zeilinger, A. V. Sergienko, and Y. Shih, New High-Intensity Source of Polarization-Entangled Photon Pairs, Phys. Rev. Lett. **75**, 4337 (1995).
[6] P. G. Kwiat, E. Waks, A. G. White, I. Appelbaum, and P. H. Eberhard, Ultrabright source of polarization-entangled photons, Phys. Rev. A **60**, R773(R) (1999).
[7] J.-W. Pan, Z.-B. Chen, C.-Y. Lu, H. Weinfurter, A. Zeilinger, and M. Żukowski, Multiphoton entanglement and interferometry, Rev. Mod. Phys. **84**, 777 (2012).
[8] J. S. Bell, On the Einstein Podolsky Rosen paradox, Physics **1**, 195 (1964).
[9] N. Brunner, D. Cavalcanti, S. Pironio, V. Scarani, and S. Wehner, Bell nonlocality, Rev. Mod. Phys. **86**, 419 (2014).
[10] B. Hensen, H. Bernien, A. E. Dréau, A. Reiserer, N. Kalb, M. S. Blok, J. Ruitenberg, R. F. Vermeulen, R. N. Schouten, and C. Abellán, *et al.*, Loophole-free Bell inequality violation using electron spins separated by 1.3 kilometres, Nature **526**, 682 (2015).
[11] M.-O. Renou, E. Bäumer, S. Boreiri, N. Brunner, N. Gisin, and S. Beigi, Genuine Quantum Nonlocality in the Triangle Network, Phys. Rev. Lett. **123**, 140401 (2019).
[12] R. Ursin, F. Tiefenbacher, T. Schmitt-Manderbach, H. Weier, T. Scheidl, M. Lindenthal, B. Blauensteiner, T. Jennewein, J. Perdigues, and P. Trojek, *et al.*, Entanglement-based quantum communication over 144 km, Nat. Phys. **3**, 481 (2007).
[13] J. Yin, Y.-H. Li, S.-K. Liao, M. Yang, Y. Cao, L. Zhang, J.-G. Ren, W.-Q. Cai, W.-Y. Liu, and S.-L. Li, *et al.*, Entanglement-based secure quantum cryptography over 1,120 kilometres, Nature **582**, 501 (2020).
[14] H. J. Briegel, D. E. Browne, W. Dür, R. Raussendorf, and M. Van den Nest, Measurement-based quantum computation, Nat. Phys. **5**, 19 (2009).
[15] M. V. Larsen, X. Guo, C. R. Breum, J. S. Neergaard-Nielsen, and U. L. Andersen, Deterministic generation of a two-dimensional cluster state, Science **366**, 369 (2019).
[16] V. Giovannetti, S. Lloyd, and L. Maccone, Quantum-enhanced measurements: Beating the standard quantum limit, Science **306**, 1330 (2004).
[17] G. Y. Xiang, B. L. Higgins, D. W. Berry, H. M. Wiseman, and G. J. Pryde, Entanglement-enhanced measurement of a completely unknown optical phase, Nat. Photon. **5**, 43 (2011).

[18] P. Komar, E. M. Kessler, M. Bishof, L. Jiang, A. S. Sørensen, J. Ye, and M. D. Lukin, A quantum network of clocks, Nat. Phys. **10**, 582 (2014).
[19] Z. Hou, Z. Zhang, G.-Y. Xiang, C.-F. Li, G.-C. Guo, H. Chen, L. Liu, and H. Yuan, Minimal Tradeoff and Ultimate Precision Limit of Multiparameter Quantum Magnetometry under the Parallel Scheme, Phys. Rev. Lett. **125**, 020501 (2020).
[20] H.-S. Zhong, Y. Li, W. Li, L.-C. Peng, Z.-E. Su, Y. Hu, Y.-M. He, X. Ding, W. Zhang, and H. Li, *et al.*, 12-Photon Entanglement and Scalable Scattershot Boson Sampling with Optimal Entangled-Photon Pairs from Parametric Down-Conversion, Phys. Rev. Lett. **121**, 250505 (2018).
[21] T. B. Pittman, B. C. Jacobs, and J. D. Franson, Single photons on pseudodemand from stored parametric down-conversion, Phys. Rev. A **66**, 042303 (2002).
[22] T. B. Pittman and J. D. Franson, Cyclical quantum memory for photonic qubits, Phys. Rev. A **66**, 062302 (2002).
[23] A. L. Migdall, D. Branning, and S. Castelletto, Tailoring single-photon and multiphoton probabilities of a single-photon on-demand source, Phys. Rev. A **66**, 053805 (2002).
[24] F. Kaneda, B. G. Christensen, J. J. Wong, H. S. Park, K. T. McCusker, and P. G. Kwiat, Time-multiplexed heralded single-photon source, Optica **2**, 1010 (2015).
[25] C. Xiong, X. Zhang, Z. Liu, M. Collins, A. Mahendra, L. Helt, M. Steel, D.-Y. Choi, C. Chae, and P. Leong, *et al.*, Active temporal multiplexing of indistinguishable heralded single photons, Nat. Commun. **7**, 10853 (2016).
[26] F. Kaneda and P. G. Kwiat, High-efficiency single-photon generation via large-scale active time multiplexing, Sci. Adv. **5**, eaaw8586 (2019).
[27] K. T. McCusker and P. G. Kwiat, Efficient Optical Quantum State Engineering, Phys. Rev. Lett. **103**, 163602 (2009).
[28] M. Gimeno-Segovia, H. Cable, G. J. Mendoza, P. Shadbolt, J. W. Silverstone, J. Carolan, M. G. Thompson, J. L. O'Brien, and T. Rudolph, Relative multiplexing for minimising switching in linear-optical quantum computing, New J. Phys. **19**, 063013 (2017).
[29] E. Lee, S. M. Lee, and H. S. Park, Relative time multiplexing of heralded telecom-band single-photon sources using switchable optical fiber delays, Opt. Express **27**, 24545 (2019).
[30] C. Zhang, Y.-F. Huang, Z. Wang, B.-H. Liu, C.-F. Li, and G.-C. Guo, Experimental Greenberger-Horne-Zeilinger-Type Six-Photon Quantum Nonlocality, Phys. Rev. Lett. **115**, 260402 (2015).
[31] J.-F. Tang, Z. Hou, Q.-F. Xu, G.-Y. Xiang, C.-F. Li, and G.-C. Guo, Polarization-Independent Coherent Spatial-Temporal Interface with Low Loss, Phys. Rev. Appl. **12**, 064058 (2019).
[32] See the Supplemental Material at http://link.aps.org/supplemental/10.1103/PhysRevApplied.19.L011002 for details of cavity adjustment, the polarization-independent optical switch, chromatic dispersion, and Refs. [41,42].
[33] E. Megidish, T. Shacham, A. Halevy, L. Dovrat, and H. S. Eisenberg, Resource Efficient Source of Multiphoton Polarization Entanglement, Phys. Rev. Lett. **109**, 080504 (2012).
[34] E. Megidish, A. Halevy, T. Shacham, T. Dvir, L. Dovrat, and H. S. Eisenberg, Entanglement Swapping between Photons That Have Never Coexisted, Phys. Rev. Lett. **110**, 210403 (2013).
[35] Z. Hou, Q. Yin, C. Zhang, H.-S. Zhong, G.-Y. Xiang, C.-F. Li, G.-C. Guo, G. J. Pryde, and A. Laing, Taking tomographic measurements for photonic qubits 88 ns before they are created, Chin. Phys. B **30**, 040304 (2021).
[36] O. Kuzucu and F. Wong, Pulsed Sagnac source of narrow-band polarization-entangled photons, Phys. Rev. A **77**, 032314 (2008).
[37] T. Nagata, R. Okamoto, J. L. O'brien, K. Sasaki, and S. Takeuchi, Beating the standard quantum limit with four-entangled photons, Science **316**, 726 (2007).
[38] L.-Z. Liu, Y.-Z. Zhang, Z.-D. Li, R. Zhang, X.-F. Yin, Y.-Y. Fei, L. Li, N.-L. Liu, F. Xu, and Y.-A. Chen, *et al.*, Distributed quantum phase estimation with entangled photons, Nat. Photon. **15**, 137 (2021).
[39] P. Walther, K. J. Resch, T. Rudolph, E. Schenck, H. Weinfurter, V. Vedral, M. Aspelmeyer, and A. Zeilinger, Experimental one-way quantum computing, Nature **434**, 169 (2005).
[40] E. Meyer-Scott, N. Prasannan, I. Dhand, C. Eigner, V. Quiring, S. Barkhofen, B. Brecht, M. B. Plenio, and C. Silberhorn, Scalable Generation of Multiphoton Entangled States by Active Feed-Forward and Multiplexing, Phys. Rev. Lett. **129**, 150501 (2022).
[41] Z.-Y. Ou, *Multi-Photon Quantum Interference* (Springer, New York, 2007), 54.
[42] J.-C. Diels and W. Rudolph, *Ultrashort Laser Pulse Phenomena* (Elsevier, San Diego, 2006), 50.